Wnt/β-catenin signaling is a novel therapeutic target for tumor suppressor CYLD-silenced glioblastoma cells

AYUMI KANEMARU[1,2*], YUKI ITO[1*], MICHIKO YAMAOKA[1*], YUKI SHIRAKAWA[3], KOU YONEMARU[1], SHUNSUKE MIYAKE[1,4], MISAKI ANDO[1], MASAKO OTA[1], TAKESHI MASUDA[5], AKITAKE MUKASA[6], JIAN-DONG LI[7], HIDEYUKI SAITO[1,4], TAKUICHIRO HIDE[8] and HIROFUMI JONO[1,4]

[1]Department of Clinical Pharmaceutical Sciences, Graduate School of Pharmaceutical Sciences, Kumamoto University, Kumamoto 860-8556; [2]Department of Development Promotion, Clinical Research Innovation and Education Center, Tohoku University Hospital (CRIETO), Sendai, Miyagi 980-8574; [3]Department of Therapy Development and Innovation for Immune Disorders and Cancers, Graduate School of Medicine, Juntendo University, Tokyo 113-8421; [4]Department of Pharmacy, Kumamoto University Hospital, Kumamoto 860-8556; [5]Department of Pharmaceutical Microbiology, Faculty of Life Sciences, Kumamoto University, Kumamoto 862-0973; [6]Department of Neurosurgery, Faculty of Life Sciences, Kumamoto University, Kumamoto 860-8556, Japan; [7]Center for Inflammation, Immunity and Infection, Institute for Biomedical Sciences, Georgia State University, Atlanta, GA 30303, USA; [8]Department of Neurosurgery, Kitasato University School of Medicine, Sagamihara, Kanagawa 252-0375, Japan

Received May 18, 2023; Accepted July 28, 2023

DOI: 10.3892/or.2023.8638

Abstract. Tumor suppressor cylindromatosis (CYLD) dysfunction by its downregulation is significantly associated with poor prognosis in patients with glioblastoma (GBM), the most aggressive and malignant type of glioma. However, no effective treatment is currently available for patients with CYLD-downregulated GBM. The aim of the present study was to identify the crucial cell signaling pathways and novel therapeutic targets for CYLD downregulation in GBM cells. CYLD knockdown in GBM cells induced GBM malignant characteristics, such as proliferation, metastasis, and GBM stem-like cell (GSC) formation. Comprehensive proteomic analysis and RNA sequencing data from the tissues of patients with GBM revealed that Wnt/β-catenin signaling was significantly activated by CYLD knockdown in patients with GBM. Furthermore, a Wnt/β-catenin signaling inhibitor suppressed all CYLD knockdown-induced malignant characteristics of GBM. Taken together, the results of the present study revealed that Wnt/β-catenin signaling is responsible for CYLD silencing-induced GBM malignancy; therefore, targeting Wnt/β-catenin may be effective for the treatment of CYLD-negative patients with GBM with poor prognosis.

Correspondence to: Dr Hirofumi Jono, Department of Pharmacy, Kumamoto University Hospital, 1-1-1 Honjo, Chuo-ku, Kumamoto 860-8556, Japan
E-mail: hjono@kuh.kumamoto-u.ac.jp

*Contributed equally

Abbreviations: CYLD, cylindromatosis; GBM, glioblastoma; GSCs, GBM stem-like cells; EMT, epithelial-mesenchymal transition

Key words: glioblastoma, CYLD, Wnt/β-catenin signaling, GBM stem-like cells

Introduction

Glioma is a malignant tumor that develops from glial cells and accounts for ~10% of all primary brain tumors. Glioblastoma (GBM) is the most aggressive type of glioma, with an extremely poor prognosis (1). Several treatments, including surgery, radiation therapy, and chemotherapy (temozolomide), are currently available for GBM (2). The combination of radiation therapy and chemotherapy (temozolomide) is the standard treatment that prolongs the survival and improves the quality of life of patients with GBM (2). However, the advantages of standard treatment are limited as recurrence is observed in most patients with GBM within one year of treatment, and their five-year survival rate is only 7.2% (3). GBM is a highly proliferative and invasive disease (4,5), and therapeutic resistance to radiation therapy and temozolomide critically contributes to the poor prognosis of affected patients (6,7). Temozolomide resistance is a major cause of GBM treatment failure (8). GBM stem-like cells (GSCs) play key roles in the therapeutic resistance of patients with GBM (9-11). As cancer stem cells are undifferentiated and self-replicating malignant cells that act as a source of cancer cells (9,10), conventional treatment with temozolomide is insufficient to inhibit GSC functions (11). Therefore, development of novel alternative treatments that suppress the malignant characteristics of GBM, including proliferation, metastasis, and GSC function, is necessary for the prognostic improvement of affected patients. However,

the detailed molecular pathogenesis and key molecules regulating the malignant transformation of cells in GBM remain unknown.

Cylindromatosis (CYLD), a tumor suppressor gene, was originally discovered as a causative gene in familial cylindromatosis (12). CYLD serves as a deubiquitinating enzyme that cleaves the Lys63-bound ubiquitin chain to regulate various cell signaling pathways (13). Previous studies have revealed that CYLD negatively controlled the activation of various signaling pathways, such as nuclear factor kappa-light-chain-enhancer of activated B cells (NF-κB) (14), transforming growth factor (TGF)-β (15,16), c-Jun N-terminal kinase (JNK) (17), and tumor necrosis factor (TNF) receptor-associated factor 2-p38 mitogen-activated protein kinase (TRAF2-p38MAPK) signaling (18), and that CYLD played important roles in various physiological processes, including immune response, inflammation, and the cell cycle, through regulating those signaling pathways (13,15,19-25). It has been reported that there is a strong association between excessive activation of signaling pathways, and the loss of CYLD function by its downregulation, in various tumors (26,27). CYLD downregulation was revealed to promote chemoresistance and invasion via NF-κB and TGF-β signaling in oral squamous cell carcinoma (16,28). Moreover, CYLD downregulation was demonstrated to be significantly associated with the malignant characteristics and poor prognosis of breast cancer (29). CYLD downregulation was also correlated with worsening grade and poor prognosis in CYLD-negative patients with GBM (30). Pathological analysis of GBM tissues has revealed that CYLD expression is reduced under hypoxic conditions, which is closely related to various malignant transformations, and that CYLD downregulation is involved in resistance to angiogenesis inhibitors (30). Despite the numerous studies strongly suggesting CYLD downregulation as a crucial factor responsible for poor prognosis, effective therapeutic targets and agents are still not available for CYLD-negative patients with GBM.

In the present study, CYLD knockdown in GBM was investigated to determine the molecular pathological mechanism of malignant transformation in CYLD-negative GBM cells and identify the crucial cell signaling pathways responsible for CYLD downregulation-dependent malignant transformation using comprehensive proteomic analysis.

Materials and methods

Antibodies and reagents. Wnt/β-catenin signaling inhibitor (ICG-001) was purchased from Selleck Chemicals. All other reagents were of the commercially available grade.

Cell lines and culture. Human GBM cell line (U251MG) was obtained from the Japanese Collection of Research Bio Resources Cell Bank. Cells were cultured in the Dulbecco's modified Eagle's medium (DMEM) with 10% heat-inactivated fetal bovine serum (FBS; both from Thermo Fisher Scientific, Inc.) at 5% CO_2 and 37˚C.

Transfection with small interfering RNA (siRNA) and plasmid DNA. For siRNA transfection, U215MG cells were incubated in a six-well plate ($2x10^5$ cells/well) or 24-well plate ($1x10^4$ cells/well) for 24 h and transiently transfected with siRNA (20 nM) using Lipofectamine® 2000 (Invitrogen; Thermo Fisher Scientific, Inc.) at 37˚C for 48 h, according to the manufacturer's protocol. Following transfection of the cells and incubation for 48 h, the experiments were performed. Silencer Negative Control siRNA (cat. no. AM4636; Ambion/Applied Biosystems; Thermo Fisher Scientific, Inc.) was used as a control (siN, https://genesdev.cshlp.org/content/suppl/2019/06/04/gad.324814.119.DC1/Supplemental_methods.pdf) (31). Sequences of the siRNAs targeting CYLD (siCYLD) were sense, 5'-GAUUGUUACUUCUAUCAAAtt-3' and antisense, 5'-UUUGAUAGAAGUAACAAUCtt-3'.

For plasmid DNA transfection, U251MG cells were incubated in a 12-well plate ($1.6x10^5$ cells/well; Corning, Inc.) at 37˚C for 24 h and transiently transfected at 37˚C for 48 h with the control vector (pcDNA3) or wild-type CYLD expression plasmid (pcDNA3) (500 ng/well) (15,32) using Lipofectamine® 2000, according to the manufacturers' protocol. The efficacy of transfections was confirmed in the present study (Fig. S1).

Cell viability assay. After 72-120 h of transfection, 50 µl/well of the Cell Counting Kit-8 solution (Dojindo Laboratories, Inc.) was added to the cells and incubated at 37˚C for 2 h, and the absorbance at 450 nm was measured using EMax SOFTmaxPRO (Molecular Devices, LLC). To evaluate the effect of ICG-001 on cell viability, cells were treated with ICG-001 (0-50 µM) and control reagent [dimethyl sulfoxide (DMSO)] in serum-free DMEM after transfection at 37˚C, and the absorbance 72 h after treatment was measured.

Transwell migration assay. Following transfection in a six-well plate, U251MG cells were recovered by trypsin addition and suspended in serum-free DMEM, and reseeded ($1.0x10^4$ cells/well) in the upper part of an 8-µm Transwell insert (Corning, Inc.) with a total volume of 200 µl/well. Cell migration was induced using DMEM containing 10% heat-inactivated FBS at a total volume of 600 µl/well. To evaluate the effect of ICG-001, ICG-001 (50 µM) or control (DMSO) with serum-free DMEM was added to the upper Transwell plate. After incubation at 37˚C for 24 h, the migrating cells were stained with crystal violet at room temperature for 20 min, and the ratio of the stained area observed by light microscope was quantified using the ImageJ software (version 1.51j8; National Institutes of Health).

Sphere-formation assay. Following transfection in a six-well plate, U251MG cells were recovered by trypsin addition and suspended in serum-free neural stem cell (NSC) medium, and reseeded ($1.0x10^4$ cells/well) in an ultra-low adhesion 96-well plate (Corning, Inc.). NSC medium including serum-free DMEM/F12, human leukemia thinner (Sigma Aldrich; Merck KGaA), human basic fibroblast growth factor (human FGF-basic; PeproTech, Inc.), human epithelial cell growth factor (human EGF; PeproTech.Inc.), heparin (Sigma Aldrich; Merck KGaA), insulin (Sigma Aldrich; Merck KGaA), N2 (Gibco), B27 (Gibco), GlutaMax (Gibco), and penicillin/streptomycin was used, as previously described (33,34). Cells with masses ≥50 µm observed by light microscope were counted as spheres.

Limiting dilution assay. Following transfection in a six-well plate, U251MG cells were recovered by trypsin addition, suspended in the NSC medium, and reseeded (1,500-2,000 cells/well) in the ultra-low adhesion 96-well plate (Corning, Inc.) using the serial dilution method. To evaluate the effect of ICG-001, after 24 h of incubation at 37˚C in NSC medium, ICG-001 (10 μM) or control (DMSO) was added to the cells, cell masses ≥50 μm were counted as spheres, and the proportion of wells in which the spheres were formed was calculated to be the percentage/4 wells after 72 h.

GBM database analysis. Patient clinical data (RNA-sequencing data of 270 samples) were obtained from a previous study (35), and RNA sequencing (RNA-seq) data were obtained from the Ivy Glioblastoma Atlas Project (GAP) database made publicly available by the Allen Institute (2015 Allen Institute for Brain Science, Ivy Glioblastoma Atlas Project 2; http://glioblastoma.alleninstitute.org/). The Ivy Glioblastoma Atlas Project is a collaborative partnership between the Ben and Catherine Ivy Foundation, Allen Institute for Brain Science, and Ben and Catherine Ivy Center for Advanced Brain Tumor Treatment. The aforementioned study provides a foundation for GBM research (35). The Ivy Glioblastoma Atlas Project provided RNA-seq data to study the gene expression patterns of anatomical structures (identified by hematoxylin and eosin staining) and cancer stem cell clusters (identified by ISH investigation) in GBM with 270 samples in both analyses combined. The expression levels of CYLD were compared with each marker or signaling-activating factor (Ki-67, fibronectin, nestin, CK2β, and CKIε) in these samples. Correlation coefficient (r) was calculated, and $|r| \geq 0.2$ indicated a correlation.

Proteomic analysis using liquid chromatograph-tandem mass spectrometry (LC-MS/MS). Whole cell lysates of U251MG cells were prepared using the phase transfer surfactant (PTS) method, as previously described (36,37). Sodium deoxycholate (SDC), sodium N-lauroylsarcosinate (SLS), ammonium bicarbonate, dithiothreitol, iodoacetamide, mass spectrometry grade lysyl endoprotease, ethyl acetate, acetonitrile, acetic acid, methanol, trifluoroacetic acid (FUJIFILM Wako Pure Chemical Corporation), modified trypsin (Promega Corporation), and 4-(2-aminoethyl) benzenesulfonyl fluoride hydrochloride (Nacalai Tesque, Inc.) were used in this study. Proteins were extracted using the PTS solution [12 mM SDC, 12 mM SLS, and 100 mM Tris-HCl (Ph 9.0)] and ultrasonically crushed for 20 min. After incubating for 5 min at 95˚C, proteins in the supernatant solution were quantified using the BCA method with the BCA Protein Assay Kit (Thermo Fisher Scientific, Inc.). The proteins were reduced with 10 mM dithiothreitol for 30 min and alkylated with 50 mM iodoacetamide in the dark for 30 min at room temperature. The protein mixture was 2-fold diluted with 50 mM ammonium bicarbonate, digested with Lys-C (1/50 sample weight) at room temperature for 3 h prior to the addition of trypsin (1/50 sample weight), and incubated at 37˚C for 20 h. An equal volume of ethyl acetate was added to the sample solution, and the mixture was acidified with 0.5% trifluoroacetic acid (final concentration). The mixture was shaken for 2 min and centrifuged at 15,600 x g for 2 min at room temperature. The upper layer was removed using a pipette and dried using a vacuum evaporator. The sample was then suspended in 100 μl buffer A (5% acetonitrile, 0.1% TFA) and desalted with GL-Tip SDB (GL Sciences, Inc.) and ODS-A-HG AAG12S50 (YMC CO., LTD.), as previously described (38,39). Peptides were eluted with buffer B (80% acetonitrile and 0.1% TFA). To concentrate the phosphorylated proteins, the Titasphere Phos-TiO Kit (GL Sciences, Inc.), was used according to the manufacturer's protocol. Subsequently, a 5% pyrrolidine solution was used for elution, as previously described (40). The eluted fraction was acidified with TFA, desalted using GL-Tip SDB, and concentrated in a vacuum evaporator. TripleTOF 5600 (SCIEX) equipped with Dionex Ultimate 3000 RSLS (Thermo Fisher Scientific, Inc.) was used for nano LC-MS/MS measurements. The injection volume was 5 μl, and the flow rate was 300 ml/min. A nanotrap column (100 μm ID, 2-cm length, packed with 5 μm Acclaim PepMap100C18; Thermo Fisher Scientific, Inc.) and an analytical nanocolumn (75 μm ID, 25-cm length, packed with 2 μm Acclaim PepMap C18; Thermo Fisher Scientific, Inc.) were used. MS data were acquired using Analyst Software TF 1.7 (SCIEX). For peptide identification, data were acquired in a data-dependent acquisition mode and analyzed using ProteinPilot 4.5 (SCIEX) connected to the UniProt human reference proteome database (Release 2017_11). Phosphorylation was set as the 'Special Factor' in the sample description. The protein identification confidence for the dataset was evaluated based on the false-discovery rate. For protein and peptide quantification, data were acquired in a data-independent acquisition mode (sequential window acquisition of all theoretical fragment ion spectra; SWATH-MS) with a variable window for the precursor ions. The proteomic datasets have been submitted to jPOSTrepo [https://repository.jpostdb.org/preview/187456970364aca64292d78; Access key: 4555; Accession no. JPST002236 (PXD043537)].

Proteomic data analysis. The results were analyzed using Kinase Enrichment Analysis 2 (https://www.maayanlab.net/KEA2/). By setting the library as 'Literature Based Kinase-Substrate Library with Phosphosites' and analyzing it using Kinase Enrichment Analysis 2, the combination of protein and phosphorylation sites was clarified. In addition, the kinases that interacted predominantly with these proteins were inferred and mapped. The results were visualized based on the Wnt/β-catenin signaling pathway-*Homo sapiens* (humans) in the Kyoto Encyclopedia of Genes and Genomes (KEGG) pathway.

Statistical analysis. Unpaired Student's t-test was used to evaluate the differences between the two groups. Statistical analysis was performed using Statcel (ver. 4; OMS Publishing Co., Ltd.). Data are presented as the mean ± standard deviation. $P<0.05$ was considered to indicate a statistically significant difference.

Results

Involvement of CYLD knockdown in the proliferation and migration of GBM cells. To develop clinically effective treatments for CYLD-negative patients with GBM, first the involvement of CYLD downregulation in the malignant characteristics of GBM cells was determined. As revealed in

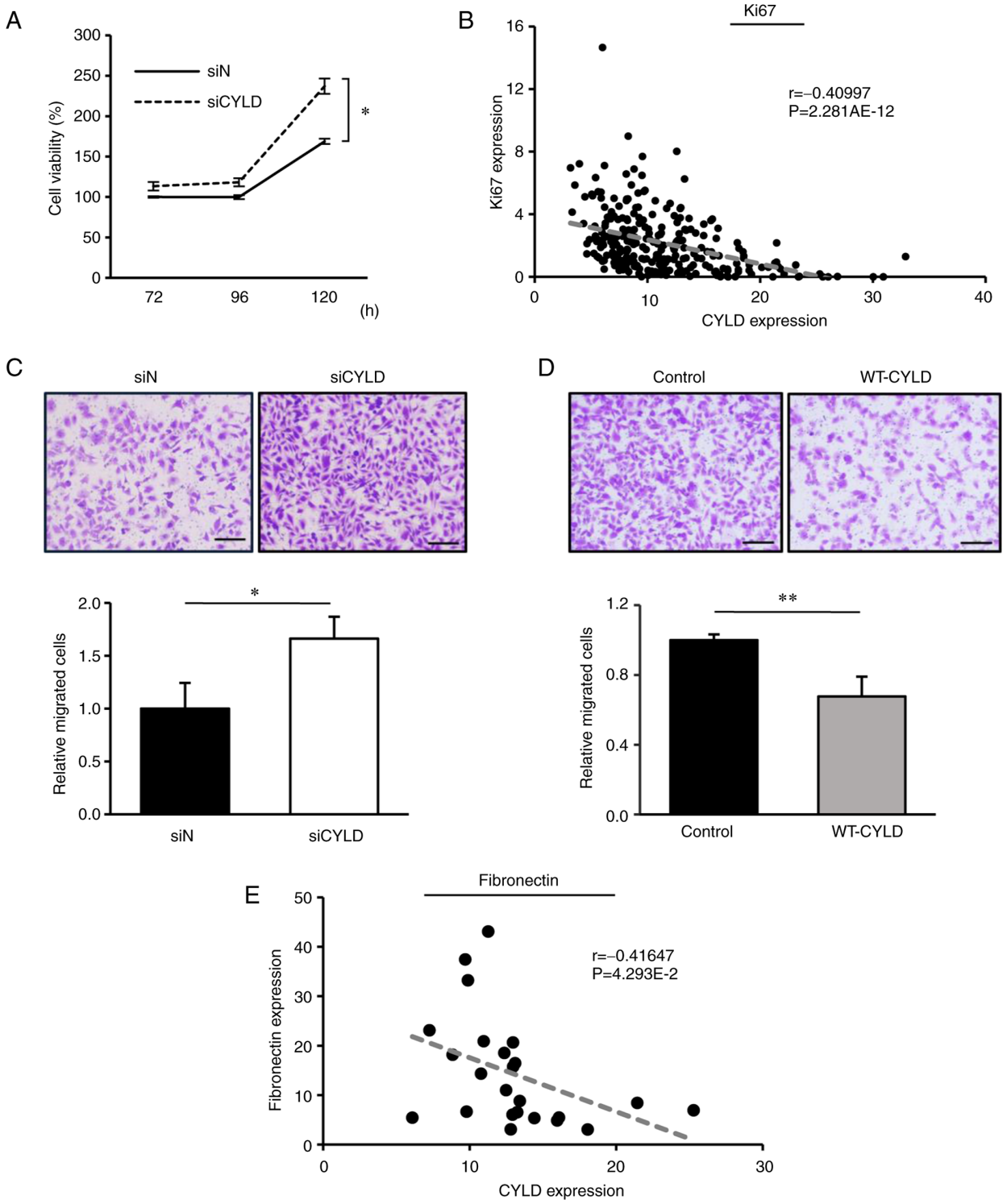

Figure 1. Involvement of CYLD knockdown in cell proliferation and migration of GBM cells. (A) Human GBM (U215MG) cells were transfected with the control siRNA (siN) or CYLD-specific siRNA (siCYLD), and cell viability was assessed 72-120 h after transfection. Values are expressed as the mean ± SD of triplicate samples. *P<0.05 vs. the siN group, via Student's t-test. (B) RNA-seq data of 270 samples using the Ivy GAP database revealed a correlation between CYLD and Ki-67 expression. The correlation coefficient is r, and the P-value indicates the significance of the correlation coefficient. (C and D) Transwell migration assays were performed using (C) CYLD-silenced and (D) CYLD-overexpressed cells. Cells were transfected, reseeded into the Transwell insert for 24 h, and migrating cells were stained with crystal violet. Scale bars, 500 μm. Values are expressed as the means ± SD. of triplicate samples. *P<0.05 and **P<0.01 vs. siN or the control group via Student's t-test. (E) RNA-seq data of 24 samples from the Ivy GAP database revealed a correlation between CYLD and fibronectin expression in the infiltrating area of GBM tissues. CYLD, cylindromatosis; GBM, glioblastoma; siRNA or si, small interfering RNA; SD, standard deviation; RNA-seq, RNA sequencing; GAP, Glioblastoma Atlas Project; WT, wild-type.

Fig. 1A, GBM cell proliferation was significantly promoted in CYLD-silenced GBM cells. Consistently, RNA-seq data obtained from the Ivy GAP database further revealed that, in the tissues of patients with GBM, CYLD expression was negatively correlated with the expression of Ki-67, a proliferation marker in GBM tissues (Fig. 1B). Next, a Transwell

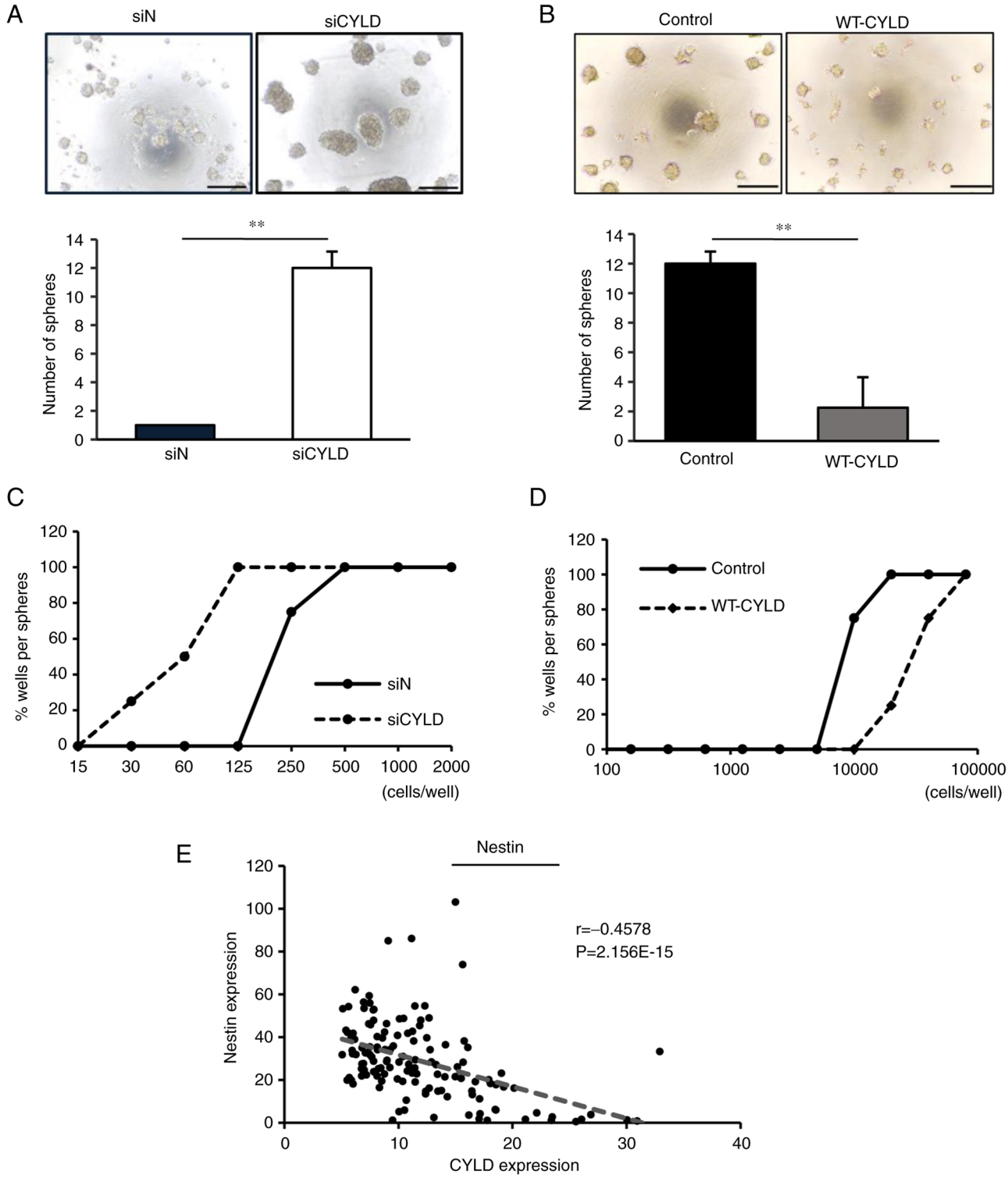

Figure 2. CYLD knockdown induces stem cell-like characteristics in glioma cells. (A and B) Sphere formation assay was performed using (A) CYLD-silenced and (B) CYLD-overexpressed cells. Cells were transfected and reseeded in the neural stem cell medium. Cell masses ≥50 μm were counted as spheres. Scale bars, 100 μm. Values are expressed as the means ± SD of triplicate samples. **P<0.01 vs. siN or the control group via Student's t-test. (C and D) Limiting dilution assay was performed using (C) CYLD-silenced and (D) CYLD-overexpressed cells. The cells were reseeded in four wells for each group. The percentage of wells in which a cell mass ≥50 μm was formed was calculated. (E) RNA-sequencing data of 135 samples from the Ivy Glioblastoma Atlas Project database revealed a correlation between CYLD and nestin expression. The correlation coefficient is r, and the P-value indicates the significance of the correlation coefficient. CYLD, cylindromatosis; si, small interfering RNA; WT, wild-type.

migration assay was performed to evaluate GBM cell migration, an epithelial-mesenchymal transition (EMT)-like change. CYLD knockdown significantly enhanced GBM cell migration (Fig. 1C), whereas CYLD overexpression markedly suppressed this effect (Fig. 1D). The Ivy GAP database further revealed a significant negative correlation between the expression levels of CYLD and fibronectin, a mesenchymal marker, in the infiltrating area of GBM tissues (Fig. 1E), indicating that

Table I. Twenty kinases identified by Kinase Enrichment Analysis 2.

Node name	Original P-value	Total genes in gene set	Total genes intersected	Intersecting genes							
CSNK1E	8.27814E-05	186	7	YWHAQ_S232	EIF4B_S597	PKP3_S238	DDX21_S171	GTF2A1_S316	SMN1_S28	SRRM2_S1326	
TAF1	0.001325212	8	2	GTF2A1_S316	GTF2A1_S321						
CSNK2A2	0.001947237	412	8	GTF2A1_S316	GTF2A1_S321	HNRNPC_S260	EIF4B_S597	RPLP1_S104	RPLP1_S101	MCRS1_S282	DDX46_S804
MAPK9	0.002454397	166	5	CTTN_T401	CTTN_S405	CTTN_S418	SLC9A1_S726	EIF3G_S42			
CAMK2A	0.019347493	100	3	EGFR_S1071	EGFR_S1081	EGFR_S1166					
MAP2K1	0.019702853	37	2	CTTN_S405	CTTN_S418						
CSNK1A1	0.027572079	115	3	YWHAQ_S232	HNRNPC_S260	HNRNPC_S253					
BCR	0.032953797	5	1	YWHAQ_S232							
PDK1	0.043737813	58	2	PDPK1_S241	PRKACA_T198						
CDC7	0.059602559	10	1	MCM2_S108							
CDK3	0.070059921	12	1	YLPM1_S634							
SGK1	0.074449031	79	2	DNAJC5_S10	EBAG9_S36						
DYRK1A	0.080403609	14	1	CCNL2_S330							
MAPK3	0.089542329	188	3	EGFR_T693	CTTN_S405	CTTN_S418					
CSNK2A1	0.095808202	435	5	GTF2A1_S316	GTF2A1_S321	HNRNPC_S260	IGF2R_S2409	MCM2_S108			
PRKCH	0.105773401	19	1	PRKD2_S710							
CSNK1D	0.113731726	102	2	YWHAQ_S232	GRLF1_S1179						
MAPK14	0.138835423	630	6	SLC9A1_S726	YLPM1_S634	TCEA1_S100	LMO7_S988	SMARCA5_S66	EGFR_T693		
CDK7	0.149726421	28	1	MCM2_S108							
CSNK1G3	0.149726421	28	1	YWHAQ_S232							

Related kinases corresponding to 44 phosphorylated proteins identified by phosphorylation proteomic analysis were included. Each P-value is dislayed in the table. CSNK1E, casein kinase 1 epsilon (CKIε); CSNK2A2, casein kinase 2, alpha prime polypeptide (CK2α); CSNK1A1, casein kinase 1 alpha 1 (CKIα).

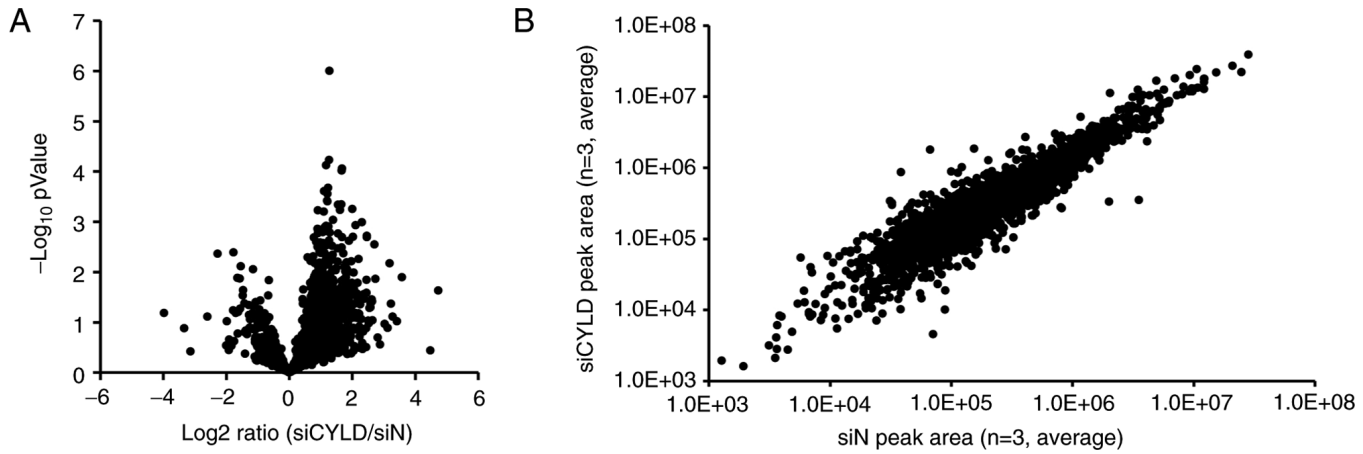

Figure 3. Comprehensive changes in phosphorylated protein expression by CYLD knockdown were assessed by proteomic analysis. (A and B) Cells were transfected with siRNA, and phosphorylated proteins were identified by enriching phosphorylated peptides and analyzing them using nano liquid chromatograph-tandem mass spectrometry. CYLD, cylindromatosis; siRNA or si, small interfering RNA.

CYLD downregulation enhanced the EMT-like changes and infiltration in GBM. These results indicated the promotion of cell proliferation and migration in CYLD-silenced GBM cells.

CYLD knockdown induces stem cell-like characteristics in glioma cells. As cancer stem cell-like cells critically contribute to malignancy in patients with GBM (41), the effects of CYLD knockdown on stem cell-like characteristics were determined in GBM cells. The sphere-forming ability, a characteristic of cancer stem cell-like cells, was evaluated. Notably, CYLD knockdown significantly increased the sphere-forming ability of GBM cells (Fig. 2A), whereas CYLD overexpression markedly suppressed this effect (Fig. 2B).

In the limiting dilution assay, CYLD-knockdown GBM cells were able to form spheres with lower cell numbers than the control GBM cells (Fig. 2C), whereas CYLD-overexpressed GBM cells required more cells (Fig. 2D). Moreover, RNA-seq data obtained from the Ivy GAP database further revealed that CYLD expression was negatively correlated with the expression of nestin, a cancer stem cell marker, in GBM tissues (Fig. 2E), suggesting that GBM cells acquire stem-like characteristics via CYLD knockdown.

Activation of Wnt/β-catenin signaling is identified in CYLD-knockdown GBM cells. To identify novel therapeutic target signals in CYLD-knockdown cells, a proteomic analysis was performed to comprehensively identify the intracellular signaling pathways involved in the malignant characteristics caused by CYLD downregulation. In total 2,914 phosphorylated proteins were identified, among which, 337 proteins were phosphorylated more than double due to CYLD downregulation (Fig. 3A and B). Kinase Enrichment Analysis 2 was used to analyze the 337 proteins. It revealed 44 combinations of proteins and phosphorylation sites, and the identified proteins were likely to interact with 20 kinases (Table I and Fig. 4A). Among the 20 kinases, 9 kinases exhibited significant differences, and the majority of them (CKIε, CK2, MAPK9, CAMK2A, and CKIα) were involved in Wnt/β-catenin signaling (Fig. 4B). RNA-seq data from the Ivy GAP database further confirmed that CYLD expression was negatively correlated with the expression of CK2β and CKIε, Wnt/β-catenin signaling activators, in GBM tissues (Fig. 4C and D). These results indicated that Wnt/β-catenin signaling plays key roles in the malignancy of cells via CYLD knockdown.

Therapeutic effect targeting Wnt/β-catenin signaling on CYLD-knockdown GBM cells. Finally, the therapeutic effects of inhibiting Wnt/β-catenin signaling on the malignant characteristics of CYLD-knockdown cells were determined. As shown in Fig. 5A and B, the promotion of cell proliferation and migration by CYLD silencing was significantly suppressed by treatment with ICG-001, a Wnt/β-catenin signaling inhibitor. Furthermore, in the limiting dilution assay, ICG-001 treatment significantly inhibited the sphere-forming ability of CYLD-knockdown GBM cells (Fig. 5C), suggesting that the inhibition of Wnt/β-catenin signaling may suppress the stem cell-like characteristics caused by *CYLD* knockdown. Taken together, the results of the present study suggest targeting Wnt/β-catenin signaling as a potential therapeutic strategy for CYLD-negative patients with GBM.

Discussion

To date, the correlation between CYLD downregulation and poor prognosis has been revealed in a variety of malignant tumors (16,29,42,43). Although effective treatments for CYLD-downregulated patients with poor prognosis have not yet been established, epidermal growth factor receptor-targeted molecular therapies are effective against CYLD-downregulated oral squamous cell carcinoma cells (44). In the present study, CYLD-silenced GBM cells were investigated and it was determined that Wnt/β-catenin signaling was significantly activated by CYLD knockdown. The results of the present study suggest that inhibiting Wnt/β-catenin signaling may be an effective therapeutic strategy for CYLD-downregulated patients with GBM with poor prognosis.

Wnt/β-catenin signaling plays important roles in cell development, regeneration, and homeostasis, and modulates the proliferation, migration, and stem cell-like characteristics of

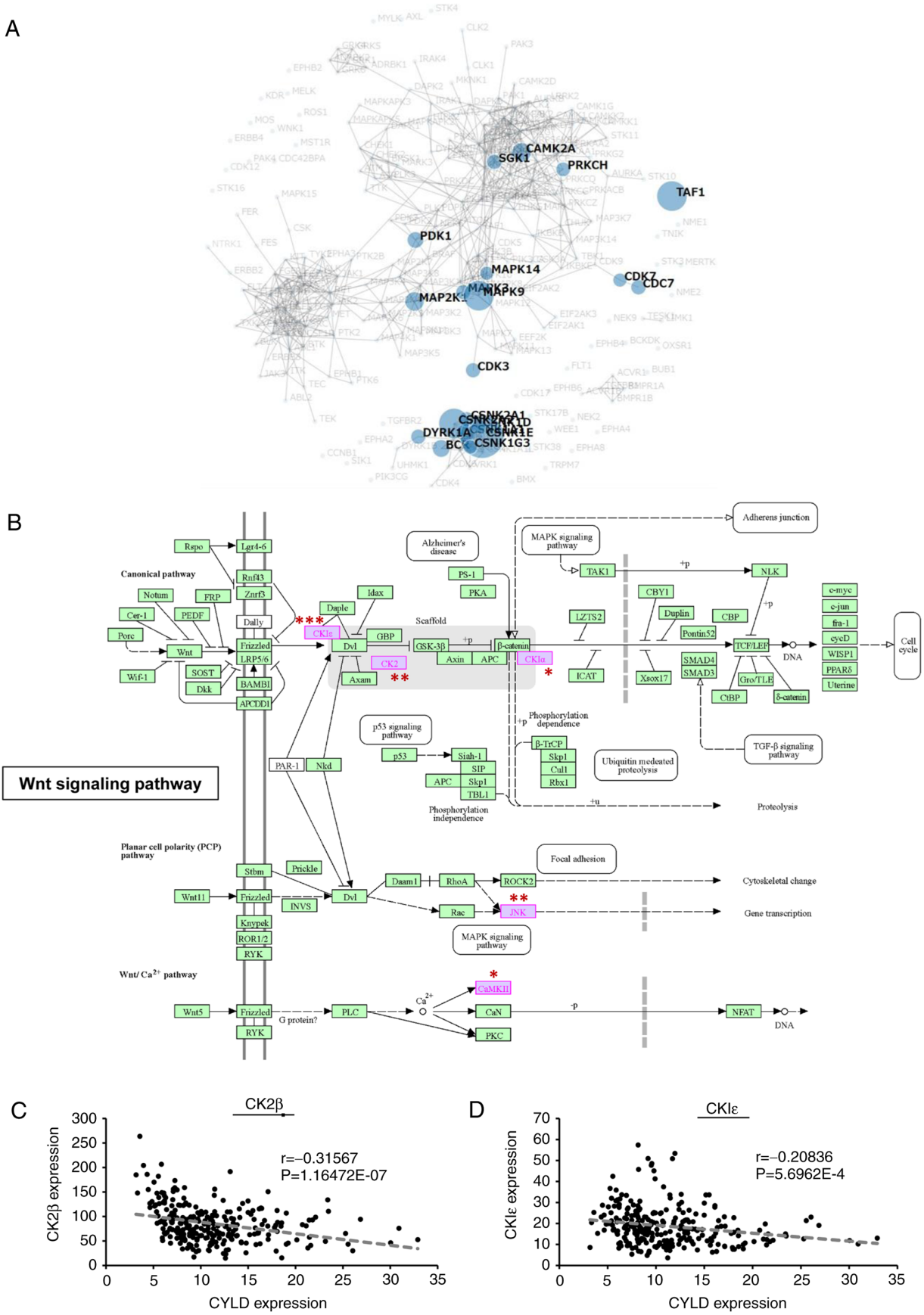

Figure 4. Activation of Wnt/β-catenin signaling is identified in CYLD-silenced glioblastoma cells. (A) Kinase Enrichment Analysis 2 was used for analysis. P-values of genes and their association with 20 kinases (listed in Table I) are displayed. (B) Among the 20 kinases, kinases involved in Wnt/β-catenin signaling were obtained using KEGG pathway analysis. The identified kinases are shown in purple. *P<0.05, **P<0.01 and ***P<0.001 via Kinase Enrichment Analysis 2 analysis. (C and D) RNA-sequencing data of 270 samples from the Ivy GAP database revealed correlations between (C) CYLD and CK2β expression and (D) CYLD and CKIε expression. The correlation coefficient is r, and the P-value indicates the significance of the correlation coefficient. CYLD, cylindromatosis; CK2β, casein kinase 2β; CKIε, casein kinase 1ε.

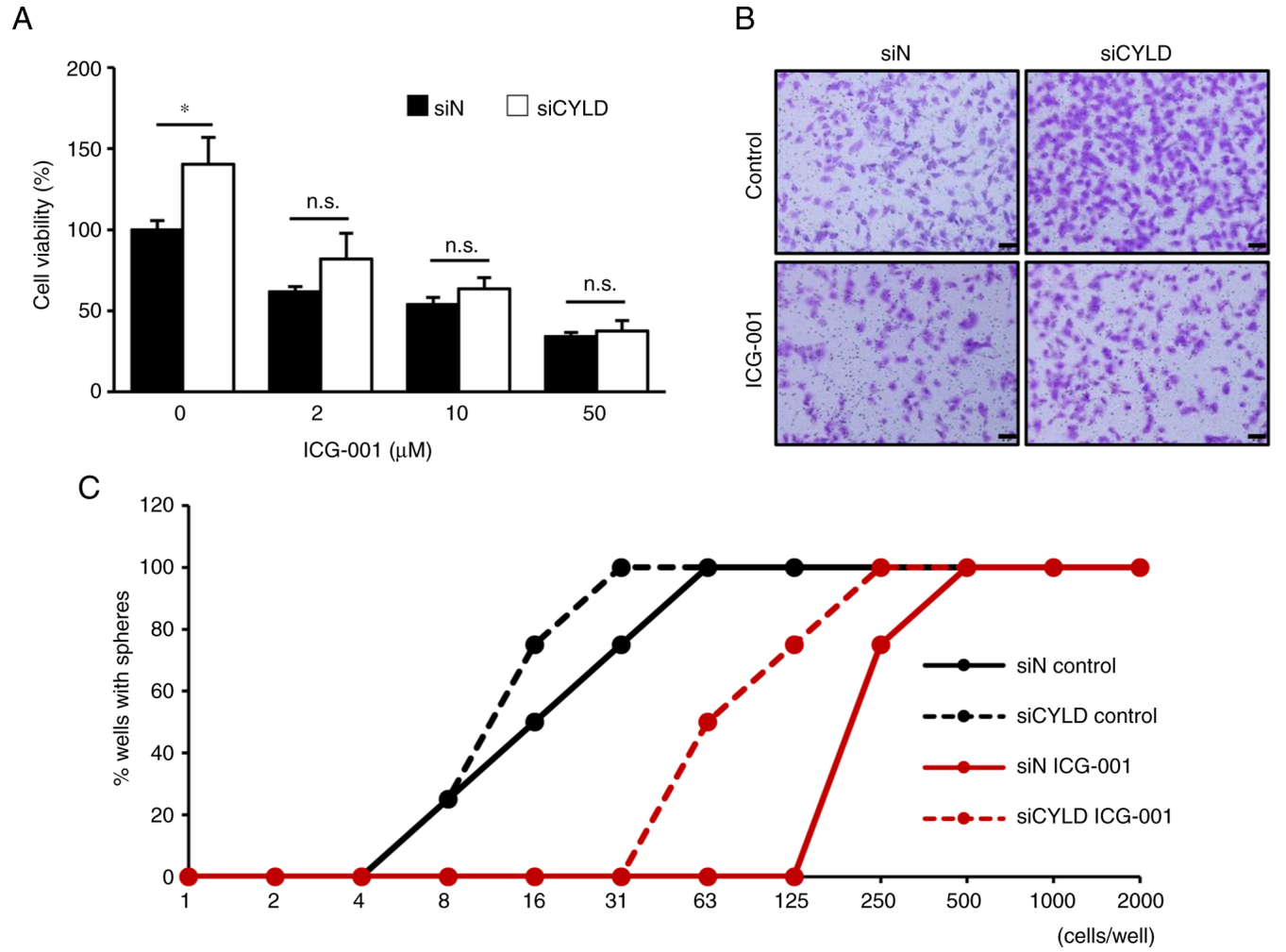

Figure 5. Therapeutic effect targeting Wnt/β-catenin signaling on CYLD-silenced GBM cells. (A) Cells were treated with ICG-001 (Wnt/β-catenin signaling inhibitor; 0-50 μM). The cell survival rate was assessed 72 h after treatment. Cell viability of the control group was considered as 100%. Values are expressed as the mean ± SD of triplicate samples. *P<0.05. (B) Cells were transfected with siRNA, reseeded into the Transwell insert with 50 μM ICG-001 or DMSO (control) for 24 h, and migrating cells were stained with crystal violet. Scale bars, 200 μm. (C) Limiting dilution assay was performed. Cells were transfected and reseeded in a cell suspension using a serial dilution method with 10 μM ICG-001 or DMSO (control). Cells were reseeded in 4 wells in each group in a 96-well plate. The percentage of wells in which a cell mass ≥50 μm was formed was calculated. CYLD, cylindromatosis; siRNA or si, small interfering RNA; DMSO, dimethyl sulfoxide; n.s., not significant.

cells (45). In GBM, Wnt/β-catenin signaling is involved in the molecular pathogenesis and progression of GBM (46-48). In the present study it was revealed that Wnt/β-catenin signaling played key roles in GBM malignant transformation caused by CYLD downregulation. Since CYLD was originally identified as a negative regulator of NF-κB signaling, numerous studies have focused on the effects of CYLD downregulation on NF-κB signaling in GBM (49-51). Song *et al* reported that CYLD suppression promotes the NF-κB signaling pathway and induces an aggressive phenotype in glioma cells (51). In addition, it was previously reported by the authors, that CYLD suppression under hypoxia promotes inflammation in GBM via NF-κB signaling (30). In the present study, both proteomic and RNA sequence analyses revealed that Wnt/β-catenin signaling, a novel critical signaling pathway, was activated and associated with CYLD downregulation in GBM (Fig. 4). Notably, all the malignant characteristics of GBM caused by CYLD knockdown were significantly suppressed by treatment with ICG-001, a Wnt/β-catenin signaling inhibitor (Fig. 5). In clinical settings, temozolomide is the only antitumor drug currently approved for GBM treatment (2). Notably, temozolomide treatment did not exert any therapeutic effects on CYLD knockdown-induced cell proliferation, migration, and GSC formation in the present study (Fig. S2), suggesting that targeting Wnt/β-catenin signaling may be a potential therapeutic strategy for CYLD-downregulated patients with GBM. Loss of CYLD expression has been revealed to enhance Wnt/β-catenin signaling via K63-linked ubiquitination of the Dishevelled (Dvl) protein (52). In the present study, KEGG pathway analysis also revealed the involvement of Dvl (Fig. 4B) in GBM, and suggested that CYLD may regulate Wnt/β-catenin signaling via the ubiquitination of Dvl. Although further investigation is necessary to clarify the precise mechanisms, including the relationship between Wnt/β-catenin and NF-κB signaling, in CYLD-downregulated GBM, Wnt/β-catenin inhibition may improve the prognosis of CYLD-downregulated patients with GBM.

Although GSCs, which exhibit chemoradiotherapy resistance and recurrence characteristics, are key prognostic factors in GBM patients (9-11), the molecular mechanisms

of GSC development remain unknown. Another interesting finding in the present study is that CYLD knockdown played key roles in development of GSCs through Wnt/β-catenin signaling. The results of the present study clearly demonstrated the impact of CYLD expression in the sphere-forming ability of GBM cells (Fig. 2). Clinical data from GBM tissues further revealed that CYLD expression was significantly associated with the cancer stem cell marker expression (Fig. 2). Moreover, Wnt/β-catenin signaling activator (CKIε) expression was correlated with CYLD expression (Fig. 4D). Consistently, a higher correlation coefficient was observed in regions with more cancer stem cells than in the entire tumor region (r=-0.235402318; data not shown). Furthermore, the expression levels of other Wnt/β-catenin signaling activators (CK2α and CK1α) were also correlated with CYLD downregulation in regions with more cancer stem cells (CK2α, r=-0.207300535; CK1α, r=-0.223871685; data not shown) in RNA-seq data. These results suggest that Wnt/β-catenin signaling, activated by CYLD knockdown, may be involved in the formation and maintenance of GSCs. As GSCs are clinically associated with chemo-radiotherapy resistance, the stem-like characteristics induced by CYLD knockdown may induce resistance to temozolomide treatment in patients with GBM (Fig. S2). In addition to the possible involvement of NF-κB signaling in GSC formation (50), the authors have previously revealed that ribosomal protein S6 (RPS6) promotes the stem-like characteristics of glioma cells (41,53,54). As RPS6 is predominantly expressed in GSC niches, concurrent with data from the Ivy GAP database, this suggests an association between CYLD and RPS6 expression. However, the detailed molecular mechanisms underlying the development and maintenance of GSCs induced by CYLD downregulation require further investigation.

The present study has some limitations. First, as the number of patients with GBM was relatively small, clinical evidence showing an association between the activation of Wnt/β-catenin signaling and CYLD expression at the protein level was limited. Second, the therapeutic effects of Wnt/β-catenin signaling inhibitor in an *in vivo CYLD*-silenced GBM model was not verified, which is necessary for the practical application of the findings of the present study. To address these limitations, the collection of more GBM specimens and the performance of *in vivo* experiments will be undertaken in future studies.

In summary, it was revealed in the present study that Wnt/β-catenin signaling was critically responsible for CYLD silenced-induced malignant characteristics, such as proliferation, migration, and GSC formation, in GBM cells. Therefore, targeting Wnt/β-catenin signaling may be a novel effective therapeutic strategy for CYLD-downregulated patients with GBM with poor prognosis.

Acknowledgements

We would like to thank Mr Shota Uchino, Ms Hitomi Arakaki, Mr Taiki Katsume, Ms Kaho Matsuyama, and Mr Yoshiki Mori (Department of Clinical Pharmaceutical Sciences, Graduate School of Pharmaceutical Sciences, Kumamoto University, Kumamoto, Japan) for their technical assistance in the present study.

Funding

The present study was supported by Grants-in-Aid for Scientific Research (B) (grant no.18H02591) to H.J. and Young Scientists (A) (grant no. 26713006) to H.J. from MEXT KAKENHI, Ministry of Education, Culture, Sports, Science, and Technology, Japan.

Availability of data and materials

The datasets used and/or analyzed during the current study are available from the corresponding author on reasonable request. The proteomics datasets have been submitted to jPOSTrepo [https://repository.jpostdb.org/preview/1874569 70364aca64292d78; Access key: 4555; Accession number: JPST002236 (PXD043537)].

Authors' contributions

TH and HJ made substantial contributions to the conception and design of the study. AK, YI and MY performed most of the experiments, acquired and analyzed the data, and confirm the authenticity of all the raw data. YS, KY, SM, MA, and MO designed the experimental procedure. TM performed the proteomic analysis using LC-MS/MS. AM, JDL and HS supervised and conceptualized the study. All the authors have read and approved the final manuscript.

Ethics approval and consent to participate

Not applicable.

Patient consent for publication

Not applicable.

Competing interests

The authors declare that they have no competing interests.

References

1. Hide T, Komohara Y, Miyasato Y, Nakamura H, Makino K, Takeya M, Kuratsu JI, Mukasa A and Yano S: Oligodendrocyte progenitor cells and macrophages/microglia produce glioma stem cell niches at the tumor border. EBioMedicine 30: 94-104, 2018.
2. Stupp R, Mason WP, van den Bent MJ, Weller M, Fisher B, Taphoorn MJ, Belanger K, Brandes AA, Marosi C, Bogdahn U, *et al*: Radiotherapy plus concomitant and adjuvant temozolomide for glioblastoma. N Engl J Med 352: 987-996, 2005.
3. Troike KM, Acanda de la Rocha AM, Alban TJ, Grabowski MM, Otvos B, Cioffi G, Waite KA, Barnholtz Sloan JS, Lathia JD, Guilarte TR and Azzam DJ: The Translocator Protein (TSPO) genetic polymorphism A147T is associated with worse survival in male glioblastoma patients. Cancers (Basel) 13: 4525, 2021.
4. Lara-Velazquez M, Al-Kharboosh R, Jeanneret S, Vazquez-Ramos C, Mahato D, Tavanaiepour D, Rahmathulla G and Quinones-Hinojosa A: Advances in brain tumor surgery for glioblastoma in adults. Brain Sci 7: 166, 2017.
5. De Barros A, Attal J, Roques M, Nicolau J, Sol JC, Cohen-Jonathan-Moyal E and Roux FE: Impact on survival of early tumor growth between surgery and radiotherapy in patients with de novo glioblastoma. J Neurooncol 142: 489-497, 2019.

6. Karachi A, Dastmalchi F, Mitchell DA and Rahman M: Temozolomide for immunomodulation in the treatment of glioblastoma. Neuro Oncol 20: 1566-1572, 2018.
7. Gujar AD, Le S, Mao DD, Dadey DY, Turski A, Sasaki Y, Aum D, Luo J, Dahiya S, Yuan L, *et al*: An NAD + -dependent transcriptional program governs self-renewal and radiation resistance in glioblastoma. Proc Natl Acad Sci USA 113: E8247-E8256, 2016.
8. Perazzoli G, Prados J, Ortiz R, Caba O, Cabeza L, Berdasco M, Gónzalez B and Melguizo C: Temozolomide resistance in glioblastoma cell lines: Implication of MGMT, MMR, P-glycoprotein and CD133 expression. PLoS One 10: e0140131, 2015.
9. Colwell N, Larion M, Giles AJ, Seldomridge AN, Sizdahkhani S, Gilbert MR and Park DM: Hypoxia in the glioblastoma microenvironment: Shaping the phenotype of cancer stem-like cells. Neuro Oncol 19: 887-896, 2017.
10. Sun H, Zhang M, Cheng K, Li P, Han S, Li R, Su M, Zeng W, Liu J, Guo J, *et al*: Resistance of glioma cells to nutrient-deprived microenvironment can be enhanced by CD133-mediated autophagy. Oncotarget 7: 76238-76249, 2016.
11. Lathia JD, Mack SC, Mulkearns-Hubert EE, Valentim CLL and Rich JN: Cancer stem cells in glioblastoma. Genes Dev 29: 1203-1217, 2015.
12. Blake PW and Toro JR: Update of cylindromatosis gene (CYLD) mutations in Brooke-Spiegler syndrome: Novel insights into the role of deubiquitination in cell signaling. Hum Mutat 30: 1025-1036, 2009.
13. Sun SC: CYLD: A tumor suppressor deubiquitinase regulating NF-kappaB activation and diverse biological processes. Cell Death Differ 17: 25-34, 2010.
14. Urbanik T, Köhler BC, Boger RJ, Wörns MA, Heeger S, Otto G, Hövelmeyer N, Galle PR, Schuchmann M, Waisman A and Schulze-Bergkamen H: Down-regulation of CYLD as a trigger for NF-κB activation and a mechanism of apoptotic resistance in hepatocellular carcinoma cells. Int J Oncol 38: 121-131, 2011.
15. Lim JH, Jono H, Komatsu K, Woo CH, Lee J, Miyata M, Matsuno T, Xu X, Huang Y, Zhang W, *et al*: CYLD negatively regulates transforming growth factor-β-signalling via deubiquitinating Akt. Nat Commun 3: 771, 2012.
16. Shinriki S, Jono H, Maeshiro M, Nakamura T, Guo J, Li JD, Ueda M, Yoshida R, Shinohara M, Nakayama H, *et al*: Loss of CYLD promotes cell invasion via ALK5 stabilization in oral squamous cell carcinoma. J Pathol 244: 367-379, 2018.
17. Reiley W, Zhang M and Sun SC: Negative regulation of JNK signaling by the tumor suppressor CYLD. J Biol Chem 279: 55161-55167, 2004.
18. Tesio M, Tang Y, Müdder K, Saini M, von Paleske L, Macintyre E, Pasparakis M, Waisman A and Trumpp A: Hematopoietic stem cell quiescence and function are controlled by the CYLD-TRAF2-p38MAPK pathway. J Exp Med 212: 525-538, 2015.
19. Jono H, Lim JH, Chen LF, Xu H, Trompouki E, Pan ZK, Mosialos G and Li JD: NF-κB is essential for induction of CYLD, the negative regulator of NF-κB. J Biol Chem 279: 36171-36174, 2004.
20. Yoshida H, Jono H, Kai H and Li JD: The Tumor suppressor cylindromatosis (CYLD) acts as a negative regulator for Toll-like Receptor 2 signaling via negative Cross-talk with TRAF6 and TRAF7. J Biol Chem 280: 41111-41121, 2005.
21. Sakai A, Koga T, Lim JH, Jono H, Harada K, Szymanski E, Xu H, Kai H and Li JD: The bacterium, nontypeable Haemophilus influenzae, enhances host antiviral response by inducing Toll-like receptor 7 expression: Evidence for negative regulation of host anti-viral response by CYLD. FEBS J 274: 3655-3668, 2007.
22. Lim JH, Stirling B, Derry J, Koga T, Jono H, Woo CH, Xu H, Bourne P, Ha UH, Ishinaga H, *et al*: Tumor Suppressor CYLD regulates acute lung injury in lethal streptococcus pneumoniae infections. Immunity 27: 349-360, 2007.
23. Lim JH, Jono H, Koga T, Woo CH, Ishinaga H, Bourne P, Xu H, Ha UH, Xu H and Li JD: Tumor suppressor CYLD acts as a negative regulator for non-typeable haemophilus influenza-induced inflammation in the middle ear and lung of mice. PLoS One 2: e1032, 2007.
24. Koga T, Lim JH, Jono H, Ha UH, Xu H, Ishinaga H, Morino S, Xu X, Yan C, Kai H and Li JD: Tumor suppressor cylindromatosis acts as a negative regulator for streptococcus pneumoniae-induced NFAT signaling. J Biol Chem 283: 12546-12554, 2008.
25. Komatsu K, Lee JY, Miyata M, Hyang Lim J, Jono H, Koga T, Xu H, Yan C, Kai H and Li JD: Inhibition of PDE4B suppresses inflammation by increasing expression of the deubiquitinase CYLD. Nat Commun 4: 1684, 2013.
26. Harsha HC and Pandey A: Phosphoproteomics in cancer. Mol Oncol 4: 482-495, 2010.
27. Massoumi R, Kuphal S, Hellerbrand C, Haas B, Wild P, Spruss T, Pfeifer A, Fässler R and Bosserhoff AK: Down-regulation of CYLD expression by Snail promotes tumor progression in malignant melanoma. J Exp Med 206: 221-232, 2009.
28. Suenaga N, Kuramitsu M, Komure K, Kanemaru A, Takano K, Ozeki K, Nishimura Y, Yoshida R, Nakayama H, Shinriki S, *et al*: Loss of tumor suppressor CYLD expression triggers cisplatin resistance in oral squamous cell carcinoma. Int J Mol Sci 20: 5194, 2019.
29. Hayashi M, Jono H, Shinriki S, Nakamura T, Guo J, Sueta A, Tomiguchi M, Fujiwara S, Yamamoto-Ibusuki M, Murakami K, *et al*: Clinical significance of CYLD downregulation in breast cancer. Breast Cancer Res Treat 143: 447-457, 2014.
30. Guo J, Shinriki S, Su Y, Nakamura T, Hayashi M, Tsuda Y, Murakami Y, Tasaki M, Hide T, Takezaki T, *et al*: Hypoxia suppresses cylindromatosis (CYLD) expression to promote inflammation in glioblastoma: Possible link to acquired resistance to anti-VEGF therapy. Oncotarget 5: 6353-6364, 2014.
31. Zemke NR, Gou D and Berk AJ: Dedifferentiation by adenovirus E1A due to inactivation of Hippo pathway effectors YAP and TAZ. Genes Dev 33: 828-843, 2019.
32. Trompouki E, Hatzivassiliou E, Tsichritzis T, Farmer H, Ashworth A and Mosialos G: CYLD is a deubiquitinating enzyme that negatively regulates NF-kappaB activation by TNFR family members. Nature 424: 793-796, 2003.
33. Balenci L, Clarke ID, Dirks PB, Assard N, Ducray F, Jouvet A, Belin MF, Honnorat J and Baudier J: IQGAP1 protein specifies amplifying cancer cells in glioblastoma multiforme. Cancer Res 66: 9074-9082, 2006.
34. Singh SK, Hawkins C, Clarke ID, Squire JA, Bayani J, Hide T, Henkelman RM, Cusimano MD and Dirks PB: Identification of human brain tumour initiating cells. Nature 432: 396-401, 2004.
35. Puchalski RB, Shah N, Miller J, Dalley R, Nomura SR, Yoon JG, Smith KA, Lankerovich M, Bertagnolli D, Bickley K, *et al*: An anatomic transcriptional atlas of human glioblastoma. Science 360: 660-663, 2018.
36. Masuda T, Saito N, Tomita M and Ishihama Y: Unbiased quantitation of Escherichia coli membrane proteome using phase transfer surfactants. Mol Cell Proteomics 8: 2770-2777, 2009.
37. Masuda T, Tomita M and Ishihama Y: Phase transfer surfactant-aided trypsin digestion for membrane proteome analysis. J Proteome Res 7: 731-740, 2008.
38. Rappsilber J, Mann M and Ishihama Y: Protocol for micro-purification, enrichment, pre-fractionation and storage of peptides for proteomics using StageTips. Nat Protoc 2: 1896-1906, 2007.
39. Rappsilber J, Ishihama Y and Mann M: Stop and go extraction tips for matrix-assisted laser desorption/ionization, nanoelectrospray, and LC/MS sample pretreatment in proteomics. Anal Chem 75: 663-670, 2003.
40. Sugiyama N, Masuda T, Shinoda K, Nakamura A, Tomita M and Ishihama Y: Phosphopeptide enrichment by aliphatic hydroxy acid-modified metal oxide chromatography for nano-LC-MS/MS in proteomics applications. Mol Cell Proteomics 6: 1103-1109, 2007.
41. Shirakawa Y, Hide T, Yamaoka M, Ito Y, Ito N, Ohta K, Shinojima N, Mukasa A, Saito H and Jono H: Ribosomal protein S6 promotes stem-like characters in glioma cells. Cancer Sci 111: 2041-2051, 2020.
42. Miyake S, Miwa T, Yoneda G, Kanemaru A, Saito H, Minoda R, Orita Y, Saito H and Jono H: Relationship between clinicopathological characteristics and CYLD expression in patients with cholesteatoma. PLoS One 15: e0240216, 2020.
43. Miyake S, Kanemaru A, Saito H and Jono H: CYLD: A novel stratification marker for malignant tumors. J Asian Assoc Sch Pharm 10: 17-22, 2021.
44. Kanemaru A, Shinriki S, Kai M, Tsurekawa K, Ozeki K, Uchino S, Suenaga N, Yonemaru K, Miyake S, Masuda T, *et al*: Potential use of EGFR-targeted molecular therapies for tumor suppressor CYLD-negative and poor prognosis oral squamous cell carcinoma with chemoresistance. Cancer Cell Int 22: 358, 2022.
45. Zuccarini M, Giuliani P, Ziberi S, Carluccio M, Iorio PD, Caciagli F and Ciccarelli R: The role of wnt signal in glioblastoma development and progression: A possible new pharmacological target for the therapy of this tumor. Genes (Basel) 9: 105, 2018.
46. Yun EJ, Kim S, Hsieh JT and Baek ST: Wnt/β-catenin signaling pathway induces autophagy-mediated temozolomide-resistance in human glioblastoma. Cell Death Dis 11: 771, 2020.

47. Boso D, Rampazzo E, Zanon C, Bresolin S, Maule F, Porcù E, Cani A, Della Puppa A, Trentin L, Basso G and Persano L: HIF-1α/Wnt signaling-dependent control of gene transcription regulates neuronal differentiation of glioblastoma stem cells. Theranostics 9: 4860-4877, 2019.
48. Zhu H, Chen Z, Shen L, Tang T, Yang M and Zheng X: Long Noncoding RNA LINC-PINT suppresses cell proliferation, invasion, and EMT by Blocking Wnt/β-Catenin signaling in glioblastoma. Front Pharmacol 11: 586653, 2021.
49. Song L, Lin C, Gong H, Wang C, Liu L, Wu J, Tao S, Hu B, Cheng SY, Li M and Li J: miR-486 sustains NF-κB activity by disrupting multiple NF-κB-negative feedback loops. Cell Res 23: 274-289, 2013.
50. Chen Z, Wang S, Li HL, Luo H, Wu X, Lu J, Wang HW, Chen Y, Chen D, Wu WT, *et al*: FOSL1 promotes proneural-to-mesenchymal transition of glioblastoma stem cells via UBC9/CYLD/NF-κB axis. Mol Ther 30: 2568-2583, 2022.
51. Song L, Liu L, Wu Z, Li Y, Ying Z, Lin C, Wu J, Hu B, Cheng SY, Li M and Li J: TGF-β induces miR-182 to sustain NF-κB activation in glioma subsets. J Clin Invest 122: 3563-3578, 2012.
52. Tauriello DVF, Haegebarth A, Kuper I, Edelmann MJ, Henraat M, Canninga-van Dijk MR, Kessler BM, Clevers H and Maurice MM: Loss of the tumor suppressor CYLD enhances Wnt/β-catenin signaling through K63-linked ubiquitination of Dvl. Mol Cell 37: 607-619, 2010.
53. Shirakawa Y, Ohta K, Miyake S, Kanemaru A, Kuwano A, Yonemaru K, Uchino S, Yamaoka M, Ito Y, Ito N, *et al*: Glioma cells acquire stem-like characters by extrinsic ribosome stimuli. Cells 10: 2970, 2021.
54. Hide T, Shibahara I, Inukai M, Shigeeda R, Shirakawa Y, Jono H, Shinojima N, Mukasa A and Kumabe T: Ribosomal proteins induce stem cell-like characteristics in glioma cells as an 'extra-ribosomal function.' Brain Tumor Pathol 39: 51-56, 2022.